P3.3

The Advanced Satellite Aviation-weather Products (ASAP) initiative at the University of Wisconsin - CIMSS

Wayne F. Feltz*, John R. Mecikalski[#], John J. Murray[+], David B. Johnson[-], Kristopher Bedka*, Sarah M. Thomas*, Anthony J. Wimmers*, Steve Ackerman*, Christopher C. Schmidt*, Mike Richards*, and Nate Ulhenbrock*

*Space Science and Engineering Center University of Wisconsin – Madison, Madison, Wisconsin

[#]Department of Atmospheric Sciences, University of Alabama, Huntsville, Alabama

[+]Langley Research Center, Atmospheric Sciences Division, Hampton, Virginia

[-]Research Applications Program NCAR P.O. Box 3000 Boulder, CO 80307

1. INTRODUCTION

A new NASA LaRC effort, the Advanced Satellite Aviation-weather Products (ASAP) initiative, has been developed to provide satellite derived meteorological products and expertise to the Federal Aviation Administration (FAA) weather research community. University of Wisconsin-Madison SSEC/CIMSS in conjunction with the University of Alabama in Huntsville, MIT, and NCAR/RAP has been tasked to provide satellite information to the NCAR-based Aviation Weather Research Program's (AWRP) Product Development Teams (PDT). Satellite derived products that ASAP will develop and provide to the AWRP PDTs are value-added information for forecasting/nowcasting aviation hazards such as those caused by low ceiling/visibility, convection, turbulence, icing, volcanic ash, and wind shear. Much of the satellite data provided to NCAR will be infused into each PDT's unique system for diagnosing a particular hazard. For ASAP in 2004 and beyond, UW will collaborate with the University of Alabama in Huntsville (see collaborating poster at conference) This collaboration will bolster UW-Madison ASAP activities by offering expertise in data mining, pattern recognition, as well as through introduction of other remote sensing data sets (e.g., lightning). Phase 2 of ASAP activities will include incorporation of hyperspectral satellite data (AIRS, CrIS, and HES) products into the FAA PDT's aviation hazard algorithms. This paper will present an overview of current University of Wisconsin-SSEC/CIMSS ASAP research and products.

2. SATELLITE CLOUD PRODUCTS

One primary focus of the ASAP initiative is the development and distribution of satellite derived cloud products to the AWRP PDT's. Currently, cloud amount, cloud top temperature, and cloud-top pressure are available from CIMSS hourly over the CONtinental United States (CONUS). These are derived using geostationary data from the Geostationary Operational Environmental Satellite (GOES)-10 (Western United States) and -12 (Eastern United States) Imager and Sounder instruments. Both the 10 km spatial resolution Sounder and the 4 km spatial resolution Imager products are derived using a multi-spectral approach, utilizing the specific spectral information provided by each instrument. An example of the GOES-12 Imager derived cloud-top height product is shown in Figure 1. Cloud-top height for the GOES-10/12 Sounder, as well as the GOES-12 Imager is derived using a combination of the IR window (Schriener *et al.,* 2001) and CO_2 absorption (Wylie and Menzel, 1989) techniques. The IR window technique is reliable for low and mid-level clouds, while the CO_2 ratio technique offers improvements in height assignment for high, semi-transparent clouds. Cloud-top heights are not produced using GOES-10 Imager data because the 13.3 μm CO_2 channel is not available on this instrument. This product is expected to have the most utility in determining where airport visibility may be limited, either currently or in the future due to the advection of clouds and/or fog.

* *Corresponding author address*: Wayne F. Feltz, CIMSS/SSEC, 1225 West Dayton Street Room 238, Madison, WI, 53706; e-mail: wayne.feltz@ssec.wisc.edu.

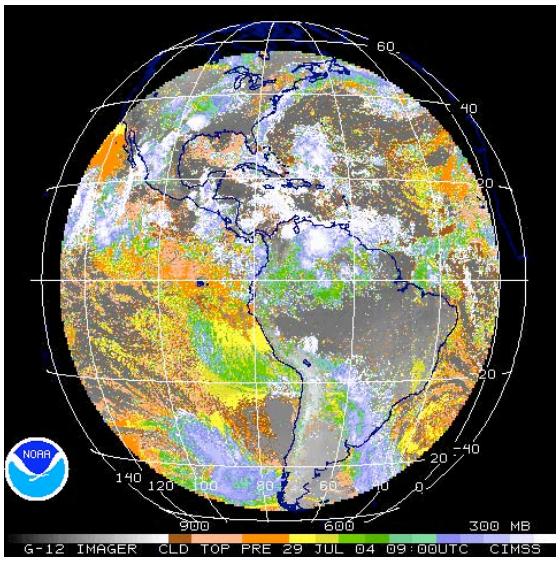

Figure 1: Sample image of cloud top pressure, derived using GOES-12 Imager data.

Validation studies have been performed using the ASAP CONUS cloud products. Specifically, the GOES-12 Imager and Sounder cloud top heights were compared to Cloud Physics Lidar (CPL) measurements from the Atlantic-THORPEX Regional Campaign (ATReC). This experiment was conducted in the winter of 2003 from Bangor, ME, and the CPL flew aboard the NASA ER-2 aircraft. Figure 2 shows the GOES-12 Imager (top- red) and GOES-12 Sounder (bottom-blue), as well as CPL (black) cloud-top heights from Dec. 05, 2003. The Imager heights show better agreement with the CPL than the Sounder heights due to the increased spatial resolution of the Imager. The best agreement for both satellite instruments is for mid-level clouds, while both the Sounder and Imager underestimate the CPL cloud-top height both for semi-transparent high clouds, and warm low-level clouds. Further validation for this product is an ongoing effort at CIMSS.

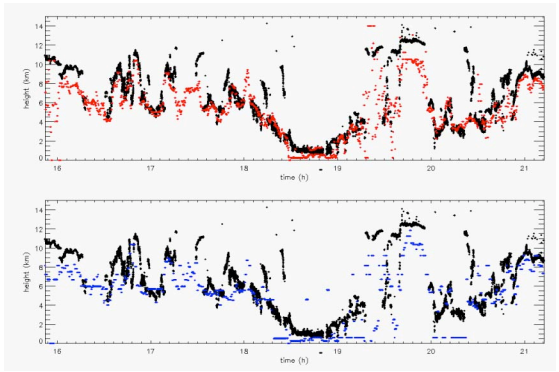

Figure 2: GOES-12 Imager (red) and Sounder (blue) cloud top height with CPL (black) cloud top height from the ATReC experiment.

In addition to the CONUS cloud products, cloud amount and cloud-top pressure are also available globally, and are derived using data from a suite of meteorological satellite instruments including GOES, MODIS, AVHRR, METEOSAT, and GMS. High temporal resolution geostationary data are used in the tropics and mid-latitudes, while the polar-orbiting AVHRR and MODIS are used to complete coverage over the polar regions. An example of the global cloud product cloud-top height is shown in Figure 3. This product uses a single wavelength (~11 μm) to determine cloud/no-cloud classifications globally. This technique is particularly useful for sensing clouds at high and mid-levels, however, sometimes miss low clouds and fog. Cloud top height is determined by comparing the ~11 μm brightness temperature (T_B) to a NWP model temperature profile. These data are expected to have the greatest utility over oceanic regions, where the lack of ground-based data is prohibitive to aviation forecasting.

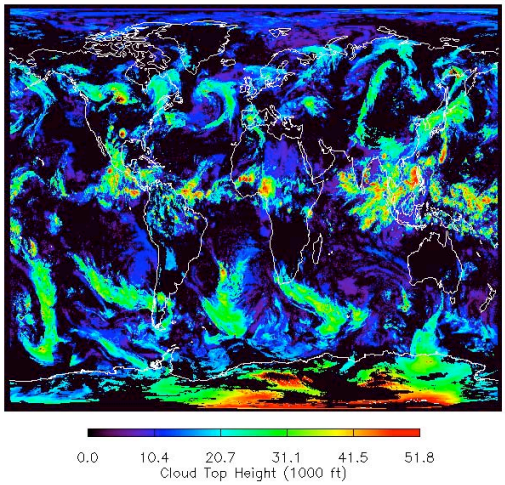

Figure 3: Sample image of cloud top height from the ASAP global cloud product.

3. CONVECTIVE PRODUCTS

Hazards related to thunderstorms (lightning, hail, strong winds and wind shear) cost the aviation industry many millions of dollars annually in lost time, fuel and efficiency through delayed, cancelled and rerouted flights, as well as accidents (Mecikalski et al. 2002; Murray 2002). Therefore, increased skill in forecasting thunderstorm initiation and evolution would be very beneficial to aviation interests.

Several products have been developed as part of the ASAP initiative to aid in the diagnosis and forecasting of convection-related aviation hazards. A classification algorithm has been developed to help identify several types of convectively-induced cloud features. This product is based upon a region growing (clustering) technique utilizing GOES visible (VIS) and multi-spectral IR data. GOES pixels are clustered based

upon statistical similarity. This classification system is produced at the 1 km GOES VIS resolution and currently identifies 5 types of convectively-induced clouds: 1) small, low-level cumulus, 2) mid-level cumulus, 3) mature cumulus clouds with depths extending through the entire troposphere, 4) thick anvil ice clouds, and 5) thin anvil and cirrus clouds. This product can be produced over both land and oceanic regions to identify potential locations of convectively-induced turbulence (CIT). This product also represents the foundation for a convective storm initiation (CI) nowcast product, for which only cumulus cloud pixels are processed, thereby reducing processing requirements and allowing for CI nowcasting over large geographical regions. An example of the convective cloud mask is shown in figure 4 for the May 4, 2003 convective storm case.

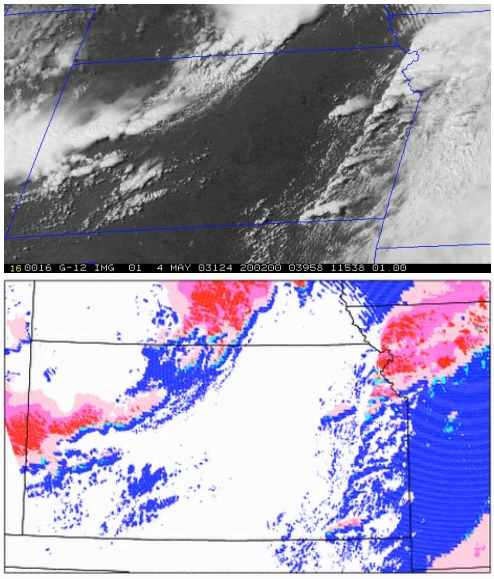

Figure 4: (top) 1 km resolution GOES-12 visible imagery at 2000 UTC on 4 May 2003. (bottom) The convective cloud classification, where blue is small low-level cumulus and thin water cloud, cyan is mid-level cumulus, red is mature cumulus, magenta is thick anvil ice cloud, and pink is thin anvil ice cloud.

Cloud-top trend estimates for moving cumulus represent the primary interest field within the CI nowcast algorithm. Roberts and Rutledge (2003) show that the occurrence of sub-freezing 10.7 μm T_B's coupled with cooling rates of 8°C/15 mins provide up to 30 mins advance notice of CI (i.e. the first detection of 35 DBz reflectivity by WSR-88D). Cloud-top cooling trends are calculated here through the use of satellite–derived atmospheric motion vectors (AMVs) produced by the UW-CIMSS algorithm (Velden et al. 1997, 1998). Figure 5 shows an example of AMVs calculated from a 3-image sequence of GOES-12 data. The UW-CIMSS algorithm was adjusted for this study to capture flow from both the synoptic- and meso-scale. AMVs within the bottom panel are associated with immature cumulus, whereas AMVs in the middle and top panels are associated with developing cumulus and mature convection, respectively. A Barnes (1964) scheme was used here to provide a complete objective analysis of the AMV field for cumulus pixels where the UW-CIMSS algorithm could not determine an AMV. A complete description of this technique can be found in Bedka and Mecikalski (2004)

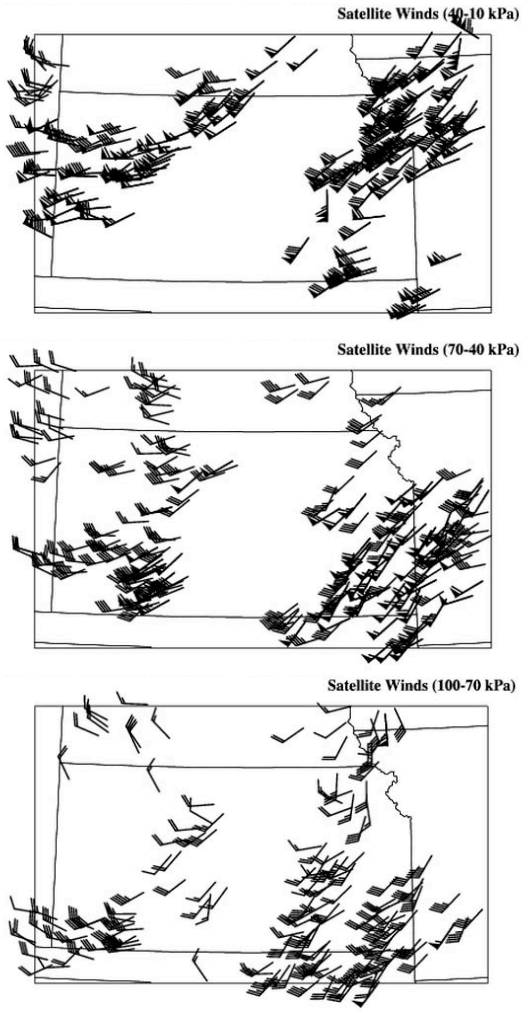

Figure 5: (top) The satellite-derived AMV field (in knots) within the 40-10 kPa layer. Only 20% of the winds are shown for clarity. (middle) Same as (top) but for the 70-40 kPa layer. (bottom) Same as (top) and (middle), but for the 100-70 kPa layer.

Through knowledge of the current AMV speed and direction, the past location of a cumulus cloud pixel can be found and cloud-top trends can be determined. The top panel of figure 6 shows an example of the 30 min 10.7 μm cumulus cloud-top cooling rates for the May 4th case. Vigorous

cumulus growth is occurring in both eastern and western Kansas, indicating that these clouds could be associated with intense CIT.

Cloud-top cooling information can be combined with several other IR-based CI interest fields to produce a CI nowcast. The bottom panel of figure 6 (bottom) shows an example of the CI nowcast product. Pixels highlighted in red meet 7 of 8 CI interest field criteria and represent cumulus for which CI should occur up to 45 mins in the future. This product can be used in flight planning to effectively direct aircraft away from locations of developing thunderstorms. A full description of this algorithm can be found in Mecikalski and Bedka (2004).

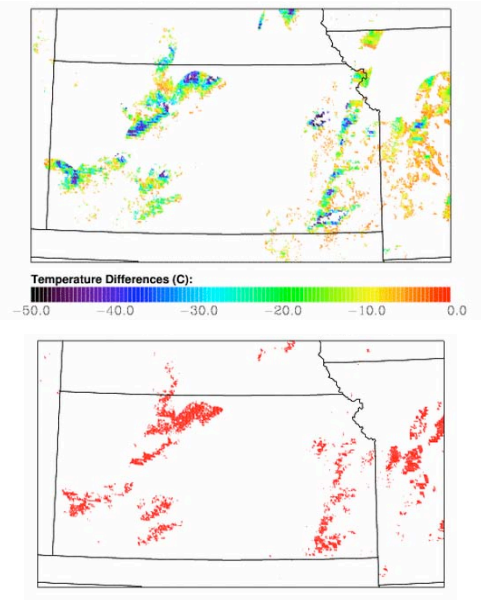

Figure 6: (top) 30-min cloud-top cooling rates for moving cumulus clouds using the AMVs shown in Figure 5. (bottom) The CI nowcast product. Pixels highlighted in red are cumulus where CI should occur 0-45 mins in the future.

4. SATELLITE TURBULENCE SIGNATURES

Turbulence presents a significant aviation hazard and can be caused by several sources. Convection, orography, and upper tropospheric instability on the synoptic-scale can all lead to significant turbulence episodes in both cloudy and "clear-air" conditions. Analysis of IR satellite data in spectral, temporal, and spatial domains is being conducted under the ASAP initiative to provide insight to possible satellite identification of turbulent regions in the atmosphere. The approach is to provide the FAA Turbulence PDT's with fields of "interest" from satellite pattern recognition and water vapor/ozone gradients.

Examples of satellite derived turbulence interest fields include a GOES water vapor gradient field which corrects for satellite viewing angle and temperature to provide a specific humidity product (Wimmers and Moody 2001, 2004), where gradients are closely correlated to tropopause folding. Figure 7 shows estimated regions of tropopause folding (grey areas), which are often associated with clear air turbulence. More information about this product can be found at:

http://cimss.ssec.wisc.edu/asap/science

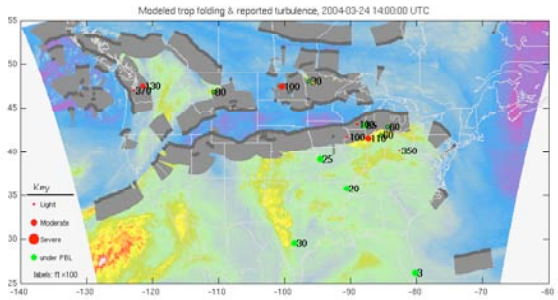

Figure 7: An example of possible regions of tropospheric folding determined through using a corrected GOES derived specific humidity field. Reports of aviation turbulence are plotted on the figure.

Another satellite-based technique is to identify and characterize regions of moderate and severe clear-air (e.g., mountain waves), and cloud-induced turbulence (e.g., thunderstorms), as detectible in GOES, and especially MODIS IR data using pattern recognition techniques. The University of Alabama-Huntsville has developed a spatial filtering methodology to identify wave structures in satellite imagery. This technique is being applied to MODIS and GOES data to provide areas of focus for possible turbulence over and downstream from mountainous regions. An example of waves existing in MODIS water vapor imagery is shown in Figure 8.

Future studies include using high vertical and spatial resolution numerical weather prediction model output containing turbulence to simulate what would be observed by future hyperspectral resolution sensors to determine if turbulence can be directly sensed with advanced high spectral resolution IR instrumentation (CrIS, IASI, HES, etc).

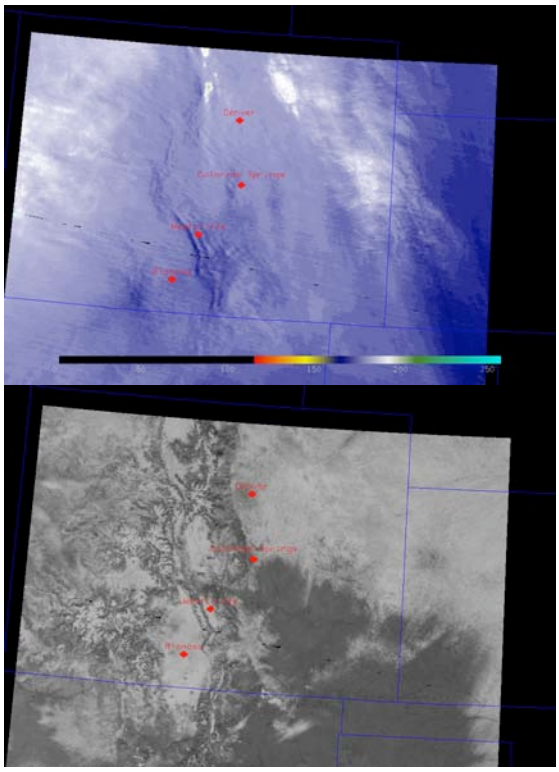

Figure 8: An example of mountain waves visible in the Terra MODIS water vapor imagery (6.7 um) but not "detected" in the visible imagery from 07 February 2004.

5. VOLCANIC ASH DETECTION

Volcanic ash has caused several nearly catastrophic commercial airline engine failures and windshield scoring incidents. Tracking post eruption ash plumes location and altitude until the cloud disperses is critical to aviation safety and economics. Geostationary satellite (GOES) sounder and imager instrumentation offers relatively good temporal resolution for the monitoring of airborne ash resulting from volcanic eruptions. While geostationary platforms provide better temporal resolution, their large fields of view and limited global coverage over volcanically active regions act as disadvantages for the tracking of volcanic ash in the atmosphere. In contrast, polar orbiting satellites (AVHRR, MODIS, GLI, and AIRS) provide high spatial resolution and better global coverage but, in general, poor temporal sampling. At any given time there are several polar orbiting satellites, each capable of detecting volcanic ash with fairly frequent time intervals at upper latitudes. This ongoing study focuses on determining how best to optimize satellite platform and IR channel selection from various IR instruments in both LEO and GEO orbits in an effort to better monitor volcanic ash (both horizontal and vertical extent) in the atmosphere.

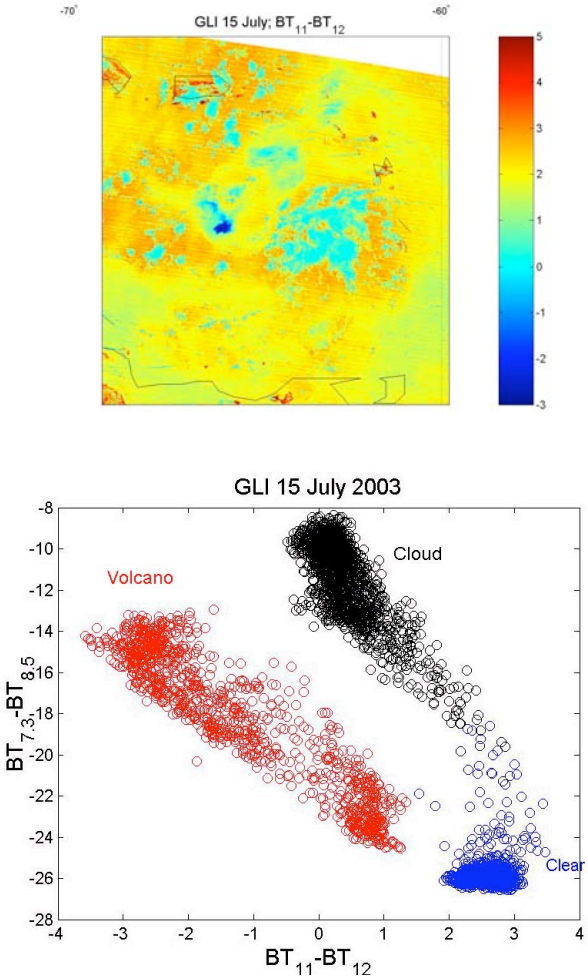

Figure 9: Japanese Global Imager data 11 – 12 um difference scene indicating the presence of volcanic ash. The 7.3 and 8.5 um differences provide a way to discriminate between volcanic ash, meteorological cloud and clear sky.

The methodology used in this research to detect the presence of volcanic ash plumes consisted of utilizing measurements from instruments onboard several polar orbiting satellites. These instruments include MODIS (Terra), AVHRR (NOAA 15, 16 and 17) and GLI (ADEOS-II). The ash detection method used is based on knowledge of spectral signatures resulting from the presence of suspended particulates. These particulates produce spectral signatures caused by differential scattering, absorption and/or emission of IR radiation by the plume constituents. The spectral signatures from the ash cloud are driven by the microphysical properties and index of refraction of the aerosols. Spectral measurements near the 11 and 12 μm channels have been successful at detecting these volcanic ash aerosols.

Detection of SO_2 can also be useful in monitoring ash clouds when SO_2 is released along with ash during a volcanic eruption. While both SO_2 and ash do not always follow the same post-eruption trajectories (Seftor et al. 1997), monitoring SO_2 clouds does provide insight for locating possible regions of volcanic ash. Considering the aforementioned spectral signature methodology, spectral measurements at 7.3 and 8.5 μm have been successful at detecting volcanic plumes containing SO_2. Both SO_2 and volcanic ash detection examples from the Soufriere Hills volcanic eruption follows.

Satellite instrumentation containing 7.3, 8.5, 11, and 12 um band spectral channels are primarily polar orbiting. GLI and MODIS provide the ability to distinguish volcanic ash, clear, and cloudy scenes from one another as presented in Figure 9. This data is useful for simulating the future geostationary Advanced Baseline Imager (ABI) capabilities set for launch after 2010.

Future work includes optimizing the operational Geostationary and Polar IR instrument (GOES and AVHRR) volcanic eruption detection algorithms to sense SO_2, volcanic ash, and plume height. In fact, good estimates of volcanic ash height are not routinely available via satellite remote sensing systems and are a major concern to the aviation community. In addition, polar research satellites (MODIS, GLI, and AIRS) will be used to provide insight for improvement of volcanic ash tracking and dissipation rates for high latitude volcanic eruptions with emphasis places on determining the altitude of the volcanic ash cloud.

The next generation geostationary IR weather instruments (ABI, GIFTS and HES) will have spectral coverage similar to existing instruments on polar orbiting satellites. This investigation, therefore, provides an opportunity to lay the ground work for future "volcanic ash detection" algorithms.

6. ACKNOWLEDGEMENTS

This research was supported by the NASA LaRC Subcontract #4400071484. More information can be found at http://cimss.ssec.wisc.edu/asap/

7. REFERENCES

Barnes, S. L., 1964: A technique for maximizing details in numerical weather map analysis. *J. Appl. Meteor.*, **3**, 396-409.

Bedka, K. M. and J. R. Mecikalski, 2004: Applications of satellite-derived atmospheric motion vectors for estimating mesoscale flows. Submitted to *J. Appl. Meteor.* (August 2004).

Mecikalski, J. R., D. B. Johnson, J. J. Murray, and many others at UW-CIMSS and NCAR, 2002: NASA Advanced Satellite Aviation-weather Products (ASAP) study report, NASA Technical Report, 65 pp. [Available from the Schwerdtferger Library, 1225 West Dayton Street, Univ. of Wisconsin-Madison, Madison, WI 53706.].

------, and K. M. Bedka, 2004: Forecasting convective initiation by monitoring the evolution of moving cumulus in daytime GOES imagery. Accepted for publication in *Mon. Wea. Rev.* (July 2004).

Murray, J. J., 2002: Aviation weather applications of Earth Science Enterprise data. Earth Observing Magazine, 11, No. 8, (August 2002).

Roberts, R. D., and S. Rutledge, 2003: Nowcasting storm initiation and growth using GOES-8 and WSR-88D data. *Wea. Forecasting*, **18**, 562-584.

Schreiner, A. J., T. J. Schmit, and W.P Menzel, 2001: Observations and trends of clouds based on GOES sounder data. *J. Geophys. Res.*, **106,** 20,349-20,363.

Seftor, C. J., N. C. Hsu, J. R. Herman, P. K. Bhartia, O. Torres, W. I. Rose, D. J. Schneider and N. Krotkov, 1997: Detection of volcanic ash clouds from Nimbus-7/TOMS, *J. Geophys. Res., 102: 16749-16760.*

Velden, C. S, C. M. Hayden, S. J. Nieman, W. P. Menzel, S. Wanzong, J. S. Goerss, 1997: Upper-tropospheric winds derived from geostationary satellite water vapor observations. *Bull. Amer. Meteor. Soc.*, **78**, 173-195.

------, T. L. Olander, and S. Wanzong, 1998: The impact of multispectral GOES-8 wind information on Atlantic tropical cyclone track forecasts in 1995. Part I: Dataset methodology, description, and case analysis. *Mon. Wea. Rev.*, **126**, 1202-1218.

Wimmers, A. J., and J. L. Moody 2001: A fixed-layer estimation of upper tropospheric specific humidity from the GOES water vapor channel: Parameterization and validation of the altered brightness temperature product, J. Geophys. Res., 106 (D15), 17115-17132.

------, and J. L. Moody, 2004: Tropopause folding at satellite-observed spatial gradients, I. Verification of an empirical relationship, J. Geophys. Res., in print.

------, and J. L. Moody, 2004: Tropopause folding at satellite-observed spatial gradients, II. Development of an empirical model, J. Geophys. Res., in print.

Wylie, D. P., and W. P. Menzel, 1989: Two years of cloud cover statistics using VAS. *J. Climate,* **2,** 380-392.